Presented at 1978 Nuclear Science Symposium,
18-20 October 1978, Shoreham-Americana Hotel,
Washington, D. C. To be published in Proc. of
IEEE Nuclear Science Symposium.

BNL 25153
Conf.-781033--40

THE TIME EXPANSION CHAMBER AND SINGLE IONIZATION CLUSTER MEASUREMENT*

A. H. Walenta

Brookhaven National Laboratory
Upton, New York 11973

October 1978

*This research was supported by the U. S. Department of Energy:
Contract No. EY-76-C-02-0016.

DISCLAIMER

THE TIME EXPANSION CHAMBER AND SINGLE IONIZATION CLUSTER MEASUREMENT*

A. H. Walenta

Brookhaven National Laboratory
Upton, New York 11973

Abstract

The time expansion chamber (TEC), a new type of drift chamber, allows the measurement of microscopic details of ionization. The mean drift time interval from subsequent single ionization clusters of a relativistic particle in the TEC can be made large enough compared to the width of the anode signal to allow the recording of the clusters separately. Since single primary electrons can be detected, the cluster counting would allow an improved particle separation using the relativistic rise of primary ionization. In another application, very high position accuracy for track detectors or improved energy resolution may be obtained. Basic ionization phenomena and drift properties can be measured at the single electron level.

Introduction

It is by now a common observation with multiwire proportional and drift chambers, that the signal waveform changes as a function of the distance between the particle trajectory and the anode wire. The most pronounced change is observed (for a particle trajectory perpendicular to the wire plane) when the particle passes at or very near the anode wire. The rise time becomes slower since the ionization distributed along the track arrives at the anode wire in a sequence given by the drift time. If the detector is operated as a drift chamber, it was found that the position resolution for tracks close to the anode degrades. In the early work on drift chambers[1,2,3] this effect has been discussed in detail. The effect was explained by the stochastic nature of the ionization in a number of ionization clusters along the track. The measured space resolution was found to be in agreement with calculations using the number of clusters obtained with the "inefficiency method", an independent measurement. In turn, the effect in the drift chamber has been used to determine the number of clusters in different gases and some results are also given in Ref. 4.

If a fast, current-to-voltage amplifier is used, the anode current is observed showing a structure with several maxima which is explained by the statistical fluctuation of the primary ionization (see e.g., Ref. 5).

It has been realized that counting the number of clusters would greatly improve the high energy particle identification based on the relativistic rise of energy loss.[6,7] The reason is that most of the relativistic rise of energy loss observed in a counter is due to the increase of the number of collisions and only little due to the change of energy loss in a single collision which corresponds here to the amount of ionization in one cluster. The latter, however, is responsible for the large fluctuations of the energy loss measurement which makes it difficult to measure the relativistic rise.

Unfortunately, in the anode current signal single clusters are not well resolved. Each peak of the structure is still composed of several clusters, since the response of the counter to a single cluster is still too slow (due to low drift velocity of positive ions) compared to the mean drift distance of the clusters in an ordinary counter.

The development of the time expansion chamber (TEC) was initiated by this problem and the solution has been found by inverting the question: instead of trying to obtain even shorter anode signals, the approach was to make the mean drift time distance between clusters large enough so that they can be distinguished.

Principle of the Time Expansion Chamber

In the TEC, the drift region is well separated from the amplification region, such that a low field can be maintained in the drift region while a normally high field is obtained in the amplification region (Fig. 1). With the choice of a suitable gas, the drift velocity in the drift region can be considerably lower than in the amplification region. In this way, the clusters of a track crossing the chamber approximately parallel to the drift field arrive at the grid in time intervals larger than in an ordinary chamber. Since the anode signal has not been slowed down, a relative time expansion has been achieved.

For best results, a number of parameters have to be optimized and some constraints on operating conditions are imposed. These parameters are given in the following list:

1. electron attachment in the low field region;
2. diffusion of clusters;
3. dependence of drift velocity on E/p;
4. number of clusters produced per cm of gas;
5. sharpness of transition from the low field region to the high field region.

Most points are related to the choice of gas, geometry, and the voltages applied.

The attachment has been studied in drift chambers, with long drift spaces (see e.g., ISIS[7,8], TPC[9,13]). It has been found that the attachment to electronegative impurities (probably O_2) is correlated to the mean agitation energy of the electrons ε such that the attachment coefficient k increases with ε decreasing. Since it is believed that the attachment process needs a catalyst (e.g., the quenching gas), one would expect the life time τ of a free electron drifting in a gas with an oxygen concentration α_1 and a quencher concentration α_2 to be described by

$$\tau \approx \frac{1}{k\alpha_1\alpha_2} \quad . \qquad (1)$$

This formula suggests that τ does not depend on the drift field once $k(\varepsilon)$, α_1 and α_2 are given. In other words, one can operate at low drift velocity and low

*This research was supported by the U. S. Department of Energy: Contract No. EY-76-C-02-0016.

drift field as successfully as in high fields if the time scale is the same. Free electron life times of the order of $\tau \approx 100$ μs have been achieved for ε only slightly higher than the thermal value in ordinary long drift distance counters and, therefore, in a TEC the attachment should be of no particular problem since the maximum drift time will be of the order of a few μs. Clearly, the correlation between k and ε may be more complex and more work is needed to clarify this point.

For a constant drift velocity v_{dr}, a mean electron energy ε, the drift field E, and a drift path s, the diffusion is given by

$$\sigma^2 = \frac{4}{3} \frac{\varepsilon}{eE} s \quad . \qquad (2)$$

This formula suggests a gas giving the smallest possible ε ($\varepsilon \approx 0.037$ eV at room temperature) at the highest possible E. The latter has to be optimized with regard to the drift velocity obtained. For the qualitative discussion, it is sufficient to use the Townsend equation for the drift velocity,

$$v_{dr} = 8.1 \frac{E}{pQ\sqrt{\varepsilon}} \ [\mathrm{cm/\mu s}] \quad , \qquad (3)$$

where E in [V/cm], p in [Torr], Q the cross section in $[10^{-16}\mathrm{cm}^2]$ and ε in [eV].

In order to obtain a low drift velocity at not too small a field, Q has to be large. On the other hand, at the 5 to 10 times higher field in the detection region, a considerably higher drift velocity is desired, which is best obtained by decreasing $Q(\varepsilon)$. Such a situation is given for gases showing the Ramsauer effect in the energy region below the minimum. Pure CH_4 would be a good choice, but for reasons connected to the gas amplification this gas did not work satisfactorily. Therefore, a mixture of Ar showing a strong Ramsauer effect and thermalizing molecular gas CH_4 + $CH_2(OCH_3)_2$ has been chosen, yet one has to be careful not to wash out the Ramsauer effect since the total cross section enters in Eq. (3).

For the first exploitation of the TEC, the gas has also been chosen such that a good detectable, not too large a number of clusters/cm is produced. According to Ref. 4, the density of the quenching gas was kept small.

The requirements for the grid are easy to fulfill. Since the field in the detection region is much stronger than in the drift region, the transparency for electrons is, by definition, high. In order to avoid uncontrolled time spread in the grid region due to the modulation of the field strength, the wire spacing has been chosen to be of the order of the spatial dimension to be resolved, i.e., the mean cluster distance of about 0.6 mm. Clearly, a mesh can be used as well for large chambers where the narrow wire spacing is impractical because of electrostatic forces.

The gap width of the detection region is smaller than in usual chambers in order to speed up the anode signal and reduce the amount and the time of arrival of the primary ionization released in this gap. This part of the signal (the first 40 ns) must be suppressed in our measurements.

Measurements

In order to reproduce anode current signals with low noise, a common base input stage has been used as described in Ref. 5, which has been modified to obtain a better rise time (τ = 4 ns). Figure 2(a) shows the response to soft x-rays from a ^{55}Fe source absorbed in the detection region. The signal has a remarkably fast trailing edge and with a slight differentiation a base width of less than 20 ns can be obtained. This has been achieved using an anode wire with a diameter of 7 μm. Figure 2(b) shows the same ionization, but for x-rays absorbed at the far end of the drift region for a high drift field (0.5 kV/cm). The time scale and sensitivity are changed by a factor of two and one half, respectively. Thus, the integrated signals allow a direct comparison, indicating within the accuracy of this method, no loss of ionization during the drift or at the grid. Comparison of the signals in Fig. 2(a) and Fig. 3(d), the latter obtained for a much smaller drift field (10 V/cm), still shows no losses. Remarkable is the decomposition of the signal into a number of single peaks at low field (Fig. 3(d)). Some of the peaks may be attributed to single electrons. The successive spread in width of the signals shown in Fig. 3(a)-(d) is attributed to diffusion and to the decrease of the drift velocity. With correction for the change of v_{dr}, the diffusion parallel to the electric field is deducted (Fig. 4). Even at very low drift fields, the spread of an ionization cluster remains small compared to the mean distance of subsequent clusters. The characteristic energy $\varepsilon_k = D/\mu$ has been calculated and is shown in Fig. 5 as a function of E/p. For E/p = 0.26, ε_k is just slightly above the thermal value as expected for this gas mixture.

Figure 6 shows the response to β-rays from a ^{90}Sr source crossing the chamber parallel to the drift field. The trigger is the signal from a scintillator behind the detection region selecting minimum ionizing particles. The sequence of individual signals during 1 μs is due to the consecutive arrival of ionization clusters from the drift region. The signal from the ionization in the detection region arrives earlier and it is not displayed.

The timing of the last visible cluster has been used to determine the drift velocity. Figure 7 shows the result as a function of E/p. For E/p = 0.26 V/cm Torr, a drift velocity of v_{dr} = 0.95 cm/μs is obtained. The drift velocity in the saturation region is $v_{dr\ sat}$ = 4.6 cm/μs, giving a time expansion factor of 4.8.

Figure 6(b) shows the same as Fig. 6(a), only the time scale has been changed. Single clusters are well separated. The signal from a single electron at this scale is about 5 mV. This approximate calibration was obtained from the pulse height of the ^{55}Fe-peak divided by the number of electrons assuming an energy of W = 28 eV for formation of one ion pair.

For the counting of single clusters, the output of the current amplifier has been slightly differentiated in order to remove the long tail. The number of clusters registered with an ordinary updating discriminator and a 100 MHz scaler (resulting dead time $\tau_D \approx 25$ ns) depends somewhat on the time constant τ_{Diff}. The best value out of three has been used (see Table 1).

Table 1

τ_{Diff}(ns)	$\bar{n}$(cm^{-1})
11	9.3
23	12.2
35	8.9

The mean number $\bar{n}$ of measured clusters per track is shown in Fig. 8 as a function of the threshold. The unit is in equivalent electrons calculated using the pulse height for the ^{55}Fe-peak as discussed above.

The statistical spread of n has been measured by recording the frequency of the occurrence for a certain n in single events for the lowest threshold (Fig. 9).

Discussion

Figure 8 shows the integral size distribution of clusters, i.e., the number of clusters greater than a given size η. This measurement, being the first of its kind, is compared to a simple theoretical model (solid line). For cluster sizes, $\eta \leq 1$ electron, the number is expected to be constant, $\bar{n}_o$ = 18 cm^{-1}, interpolating independent measurements (Ref. 4). Using the simple Rutherford cross section, the number of single collisions $N_{>\varepsilon}$, with an energy loss $\Delta E > \varepsilon$, is given by

$$N_{>\varepsilon} = \frac{ax}{\varepsilon} \qquad (4)$$

with $ax = 0.153\ 1/\beta^2\ Z/A\ \rho x$, ρ the density and x the length of the absorber. Assuming the size of the clusters proportional to the energy loss $\eta \sim \Delta E$, one obtains for the number of clusters greater than η,

$$\bar{n}_{>\eta} = \frac{\bar{n}_o}{\eta} .$$

The comparison to the measurement shows that for low threshold, the measured value is too small which can be explained by the dead time loss determined by the single cluster pulse width and the response of the discriminator. For larger cluster size, the deviation may be due to saturation effects of the gas gain. The relatively small increase of $\bar{n}$ for values $\eta < 1$ e indicates that single electrons are detected rather efficiently.

Particle Separation Using the Relativistic Rise

Figure 9 shows the statistical fluctuation of n measured for single tracks. The solid line represents a Gaussian with $\sigma = \sqrt{\bar{n}}$ where $\bar{n}$ = 12.2 is the measured value. This good agreement allows the extrapolation towards a large system, as for particle identification, using the relativistic rise of $\bar{n}$. Counting the total number of clusters over a track length of 1.3 m, by adding the numbers of conveniently smaller subsamples, yields $\bar{n}_{tot}$ = 1600 with a variance of σ = 2.5%. The difference of $\bar{n}$ for pions and kaons in the region of relativistic rise is expected to be only slightly smaller than for the energy loss. Thus one would expect a π/K separation of about 6σ, a value about twice as good as obtained measuring the integrated pulse height (Ref. 10). Clearly, a reduction of the dead time for cluster counting and an increase of the number of detected clusters per cm to about $\bar{n}$ = 30 cm^{-1}, using a different gas, is within the reach of the present techniques and would improve the result even further.

Two simple illustrative arguments can be found for the improvement compared to the pulse height measurement. The pulse height distribution in the same counter has a full width at half maximum of 100%, while the distribution of $\bar{n}$ gives a full width at half maximum of 67%. Furthermore, in the measurement with a number of cells m, the resolution improves for the pulse height measurement as $m^{0.428}$, but for the cluster counting as $m^{0.5}$ which gives a factor 1.42 at m = 130.

Low Energy Radiation Measurement

The diffusion and the very large time expansion at low fields (see e.g., Fig. 3(d)) suggests the use of the TEC for the detection of low energy radiation ($E \leq 1$ keV) with good energy resolution having the advantage of higher speed, providing a position resolution and large surface as compared to semiconductor detectors.

A radiation (x-rays, electrons) with an energy of about 1 keV releases ca 30 single electrons which may be detected and counted individually in the TEC. With a Fano factor F = 0.2, an energy resolution of 19% FWHM could be expected since the statistical fluctuation of the proportional gas gain is eliminated.

The systematic study of Fano factors in gases is possible. If theoretical values $F \leq 0.1$ and $W \approx 20$ eV can be verified (Penning mixtures), resolutions of 10% FWHM should be possible for 1 keV radiation.

Position Resolution

Briefly, the possibility of improved position resolution should be mentioned (Track B, Fig. 1). The analysis of the ultimate position resolution obtained in drift chambers (Ref. 4) indicates three obstacles for further improvement:

1. statistical fluctuation of primary ionization;
2. diffusion;
3. limited speed of anode signal.

The third point is easily improved by the TEC since the speed of the anode signal remains the same but the drift time scale is expanded. Points 1 and 2 normally can be improved by providing a denser ionization, which is for minimum ionizing particles only possible by increasing the gas density, which has practical limits. Increasing the amount of ionization by increasing the gap thickness and measuring an appropriate mean of the leading edge of the anode signal gives no improvement, since only the first cluster arriving at the anode has a definite geometrical meaning which is the shortest distance between the track and the anode. The later arriving clusters do not contain useful time information because they don't follow straight field lines and are, due to their random distribution along the track, also randomly delayed. In the TEC, however, this time spread caused by the radial field around the anode wire is small ($\Delta t \leq 5$ ns) and corresponds, with the small drift velocity v_{dr}, to a small position error $\Delta X_r = v_{dr} \cdot \Delta t$. Adding the effect of diffusion ΔX_D, a position resolution of $\Delta X \approx \sqrt{\frac{(v_{dr}\Delta t)^2 + \Delta X_D^2}{n}}$ can be reached with n, the number of detected clusters. Values of $\Delta X \leq 10$ µm seem possible. Neglecting a short and almost constant delay, the grid

can be considered as a "virtual amplification plane".

Conclusion

The TEC represents a new tool suitable for extended study of the ionization process (δ-rays, low energy electron range, Fano-factor, W-values, etc.) for study of the drift process (shape of charge distribution parallel to the drift field, drift velocity at very low fields).

The TEC provides, also, a new tool for practical applications where very high position resolution or double track resolution is needed. Improved energy resolution for quanta can be obtained, since the fluctuation of gas gain is absent in the single electron counting mode and the considerable improvement for mass determination of relativistic particles is obvious.

Acknowledgement

I wish to thank Dr. J. Fischer and Dr. V. Radeka for their support, interest, and many helpful discussions. The discussions with A. Hrisoho and his contribution to the development of the idea of low energy radiation measurement are acknowledged as well as his help in the modification of the amplifier.

References

1. A. H. Walenta, Nucl. Instr. & Meth. 111 (1973) 467.
2. A. H. Walenta, "Driftkammern", GSI Bericht P3-74, Arbeitstagung über Detektoren, Darmstadt, July 1973.
3. K. O. Greulich, "Einfluß von Zählgasgemischen auf Driftzeitkurven und Driftzeitverteilungen in einer Vieldraht Driftkammer", Diplomarbeit, Heidelberg, 1973.
4. W. Farr, J. Heintze, K. H. Hellenbrand, and A. H. Walenta, Nucl. Instr. & Meth. 154 (1978) 175.
5. V. Radeka and P. Rehak, IEEE Trans. Nucl. Sci., NS-25, (1978) 46.
6. V. A. Davidenko, B. A. Dolgoshein, V. K. Semenov, and S. V. Somov, Nucl. Instr. & Meth. 67 (1969) 325.
7. J. H. Cobb, W. W. M. Allison, and J. N. Bunch, Nucl. Instr. & Meth. 133 (1976) 315.
8. J. H. Cobb, "A Study of Some Electromagnetic Interactions of High Velocity Particles with Matter", Thesis, Oxford (1975).
9. "Proposal for a PEP Facility Based on the Time Projection Chamber (TPC)", LBL-UCLA-Yale-Riverside-Johns Hopkins, December (1976).
10. A. H. Walenta, J. Fischer, H. Okuno, and C. L. Wang, to be published.
11. L. W. Cochran and D. W. Forester, Phys. Rev. 126 (1962) 1785.
12. G. Schulz and J. Gresser, Nucl. Instr. & Meth. 151 (1978) 413.
13. N. Hadley, D. Pollard, and P. Robrish, September 20, 1977, TPC-LBL-77-23; N. Hadley, P. Robrish, and D. Pollard, December 15, 1977, TPC-LBL-42; P. Robrish, N. Hadley, G. Przybylski, and F. Brown, October 16, 1978, TPC-LBL-78-60.

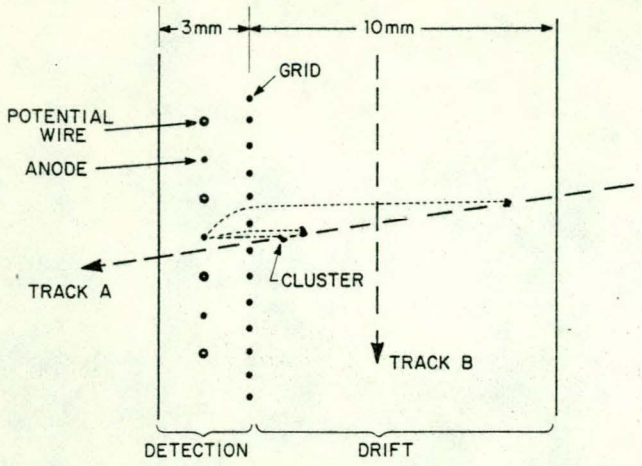

Fig. 1. Electrode arrangement and principle of the TEC. Track A for ionization loss measurement, track B for position measurement.

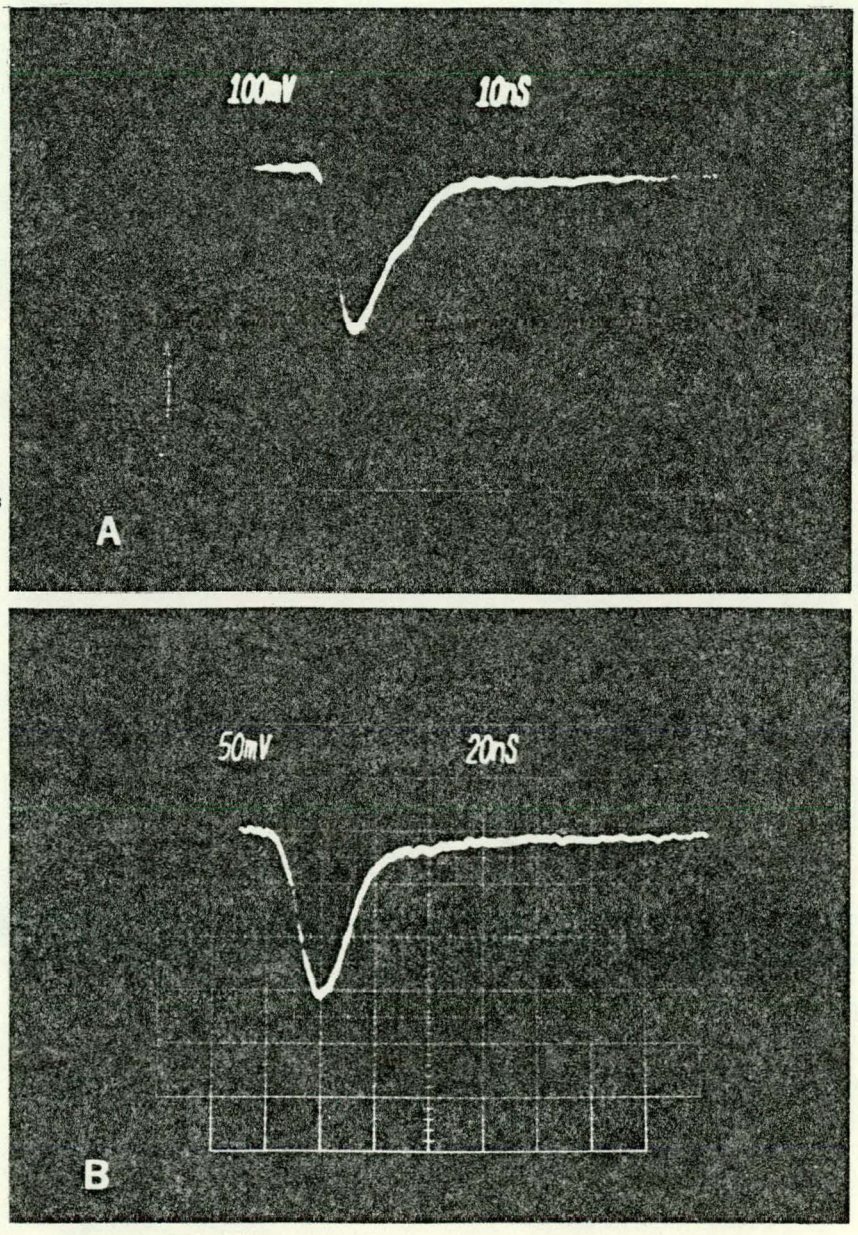

Fig. 2. Signals after the current-to-voltage preamplifier for ^{55}Fe. Step response rise time of the preamplifier was 4 ns.

(a) Quantum absorbed in detection region.

(b) Quantum absorbed at the far end of drift region.

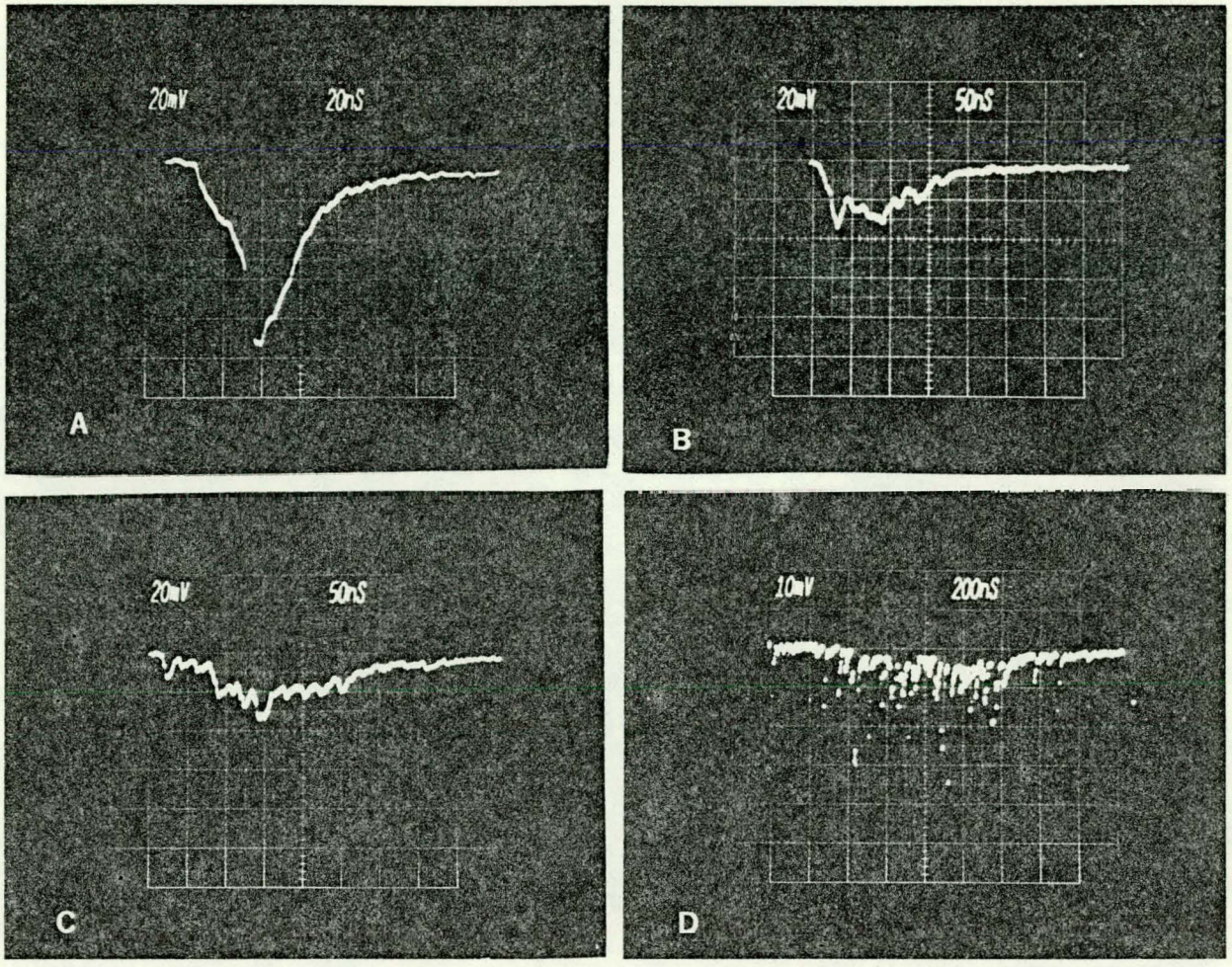

Fig. 3. Signals for ^{55}Fe x-rays absorbed at the far end of the drift region.

(a) E = 200 v/cm (c) E = 50 v/cm

(b) E = 100 v/cm (d) E = 10 v/cm

For (d), the gas gain had been increased.

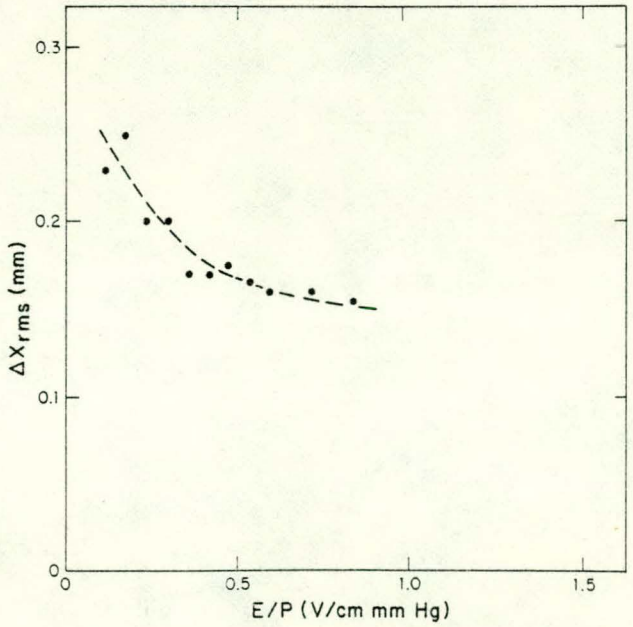

Fig. 4. ΔX_{rms} due to diffusion parallel to E.

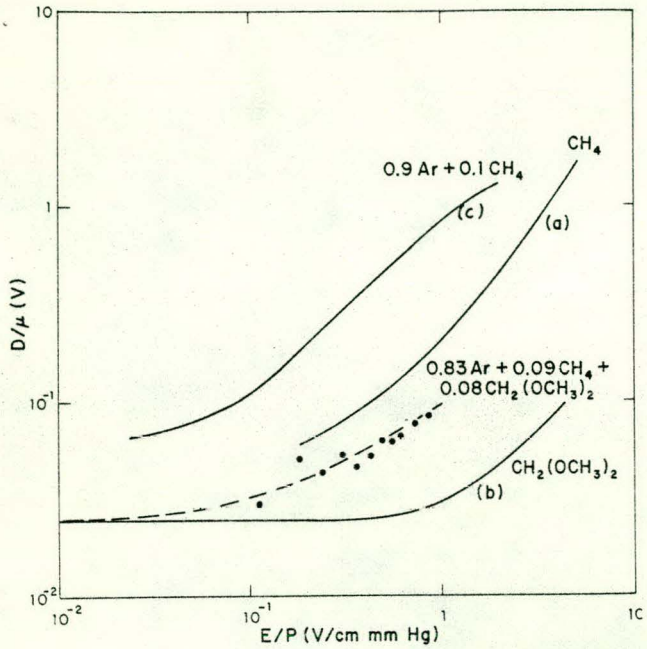

Fig. 5. Characteristic energy D/μ

(a) measurement [11]

(b) calculated [12]

(c) calculated [2,3]

(•) measurement for the mixture

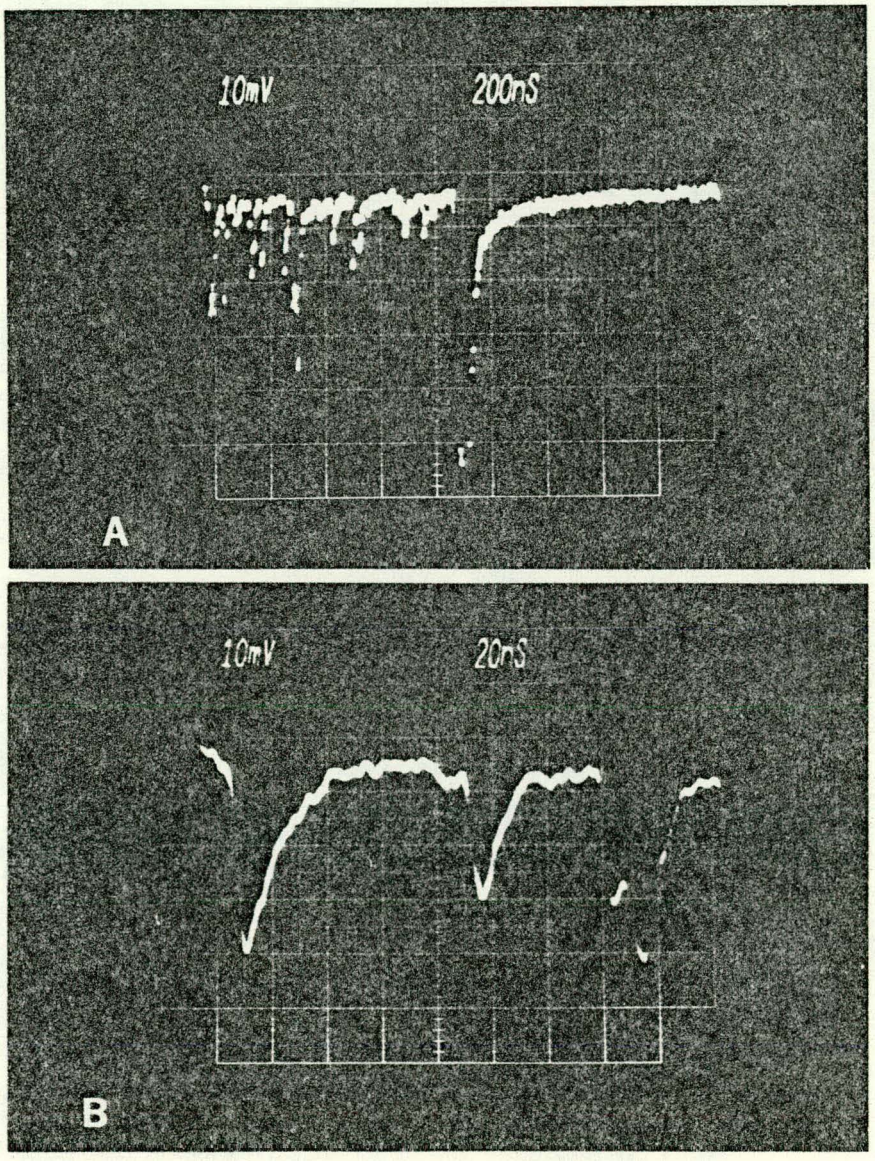

Fig. 6. Signal for a single β^- (^{90}Sr) crossing the chamber (track A, Fig. 1), drift field E = 200 v/cm

(a) full scale;

(b) expanded view

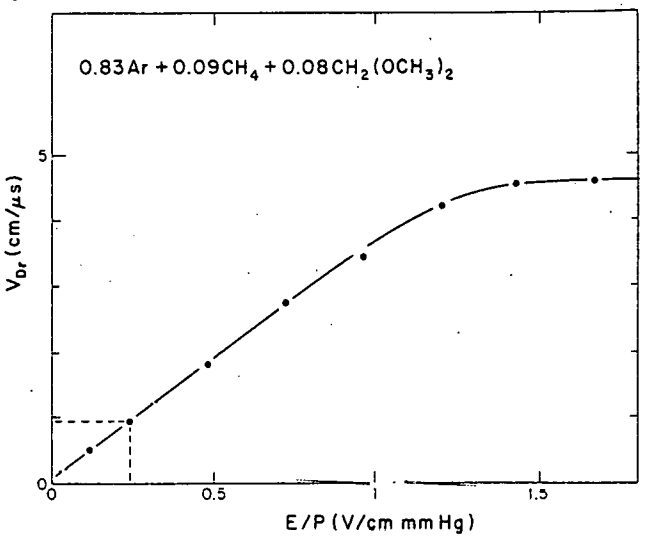

Fig. 7. Drift velocity as a function of reduced field strength.

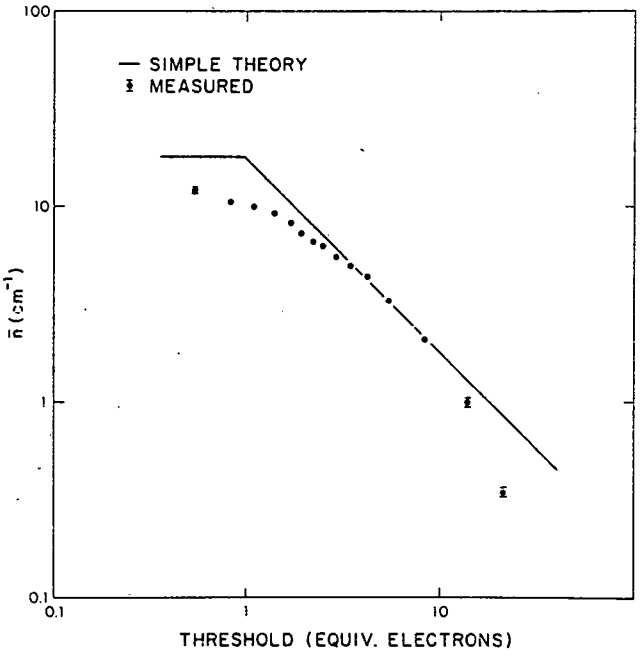

Fig. 8. Mean number of registered clusters as a function of threshold.

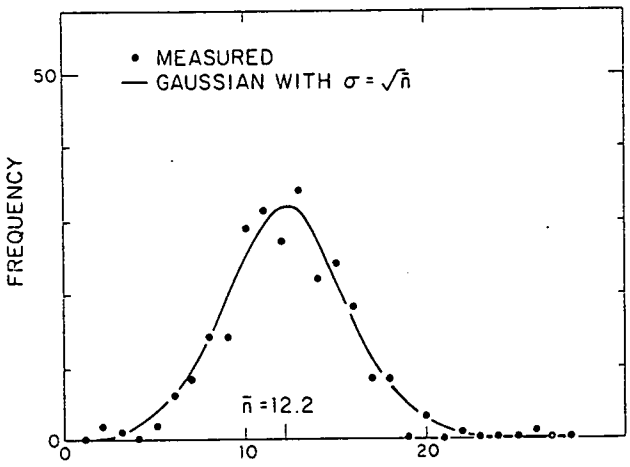

Fig. 9. Frequency of measured number of clusters per track.